Geological Society of America
Special Paper 356
2002

Dating the end-Triassic and Early Jurassic mass extinctions, correlative large igneous provinces, and isotopic events

József Pálfy*
Hungarian Natural History Museum, P.O. Box 137, H-1431, Budapest, Hungary
Paul L. Smith
James K. Mortensen
Department of Earth and Ocean Sciences, University of British Columbia, Vancouver, British Columbia V6T 1Z4, Canada

ABSTRACT

The end-Triassic marks one of the five biggest mass extinctions, and was followed by a well-known second-order extinction event in the Early Jurassic. Previously published geological time scales were inadequate for correlation of extinctions with other global events and to unravel their dynamics. Here we present a revised time scale based on high-precision U-Pb ages integrated with ammonoid biochronology resolved to the zone level. This compilation suggests that the end of the Triassic Period (ca. 200 Ma) coincided with peak volcanism in the Central Atlantic magmatic province and that terrestrial floral and faunal extinctions may have slightly preceded the marine biotic crisis. The $^{87}Sr/^{86}Sr$ and $\delta^{13}C$ stratigraphic records are compatible with volcanically induced global environmental change that could be the proximal cause of extinction.

The revised Early Jurassic time scale suggests that peak extinction in the early Toarcian occurred at 183 Ma. Recent isotopic dating of flood basalts from the southern Gondwanan Karoo and Ferrar provinces documents a synchronous culmination in volcanic activity at 183 ± 2 Ma. The onset of volcanism is correlative with the start of a rapid rise in seawater $^{87}Sr/^{86}Sr$ ratios. A recently recognized negative $\delta^{13}C$ anomaly, tentatively ascribed to a massive release of methane hydrate, and the subsequent widespread oceanic anoxia suggest that the environmental perturbations thought to trigger the extinction also seriously disrupted the global carbon cycle. The interval between these two extinctions is 18 m.y., significantly shorter than the hypothetical 26 m.y. periodicity of extinctions.

INTRODUCTION

The Mesozoic era is framed by the two most studied mass extinctions, the end-Permian and Cretaceous-Tertiary events. Much less research effort has been devoted to two other events that occurred in the first half of the Mesozoic, i.e., at the close of Triassic and in the Early Jurassic. The end-Triassic mass extinction is the least studied and most poorly understood event among the five major mass extinctions (Hallam, 1996a). A subsequent extinction in the Early Jurassic, a second-order event

*E-mail: palfy@paleo.nhmus.hu

Pálfy, J., Smith, P.L., and Mortensen, J.K., 2002, Dating the end-Triassic and Early Jurassic mass extinctions, correlative large igneous provinces, and isotopic events, *in* Koeberl, C., and MacLeod, K.G., eds., Catastrophic Events and Mass Extinctions: Impacts and Beyond: Boulder, Colorado, Geological Society of America Special Paper 356, p. 523–532.

close to the Pliensbachian-Toarcian boundary, is one of the better known minor events (Harries and Little, 1999). However, a common impediment to the reconstruction of these crises and identification of their causes is the inadequate knowledge of their timing, due to the poor calibration of the latest Triassic and Early Jurassic time scale.

Extraterrestrial impacts, climate changes, sea-level changes, oceanic anoxia, and flood basalt volcanism are among the most frequently cited agents that could lead to elevated extinction rates or ecosystem collapse. In each case, testing of competing hypotheses requires precise timing and correlation of events. A recent revision of the Jurassic numerical time scale employed high-precision U-Pb zircon or $^{40}Ar/^{39}Ar$ geochronology of volcanic-ash layers embedded in fossiliferous sedimentary rocks (Pálfy et al., 2000b). Herein we review the new timing limitations of early Mesozoic extinctions in order to gain new insights into their potential causes.

The ramifications of the refined time frame have been discussed elsewhere for the end-Triassic (Pálfy et al., 2000a) and early Toarcian events (Pálfy and Smith, 2000). In this chapter we compare the two events and cite evidence for the synchronicity of extinctions and pulses of flood basalt volcanism. Temporal relationships between biotic crises and flood basalt volcanism in the Central Atlantic magmatic province and the Karoo-Ferrar igneous province are analyzed using a summary of recently published isotopic dates for the two large igneous provinces. Synchrony suggests possible causal relationships, as proposed earlier (e.g., Rampino and Stothers, 1988; Courtillot, 1994). If volcanically triggered environmental perturbations were the driving force of these extinctions, then distinctive isotopic signatures are expected in the stratigraphic record and can be used to test hypotheses. Therefore we also assess the compatibility of such scenarios with recent isotopic data.

RADIOMETRIC DATING OF EARLY MESOZOIC EXTINCTIONS

The accuracy of numerical time scales commonly used in the 1990s (e.g., Harland et al., 1990; Gradstein et al., 1994; Fig. 1) is compromised by several problems: (1) they are based on a small number of isotopic ages, (2) many of the isotopic ages were produced by K-Ar and Rb-Sr dating methods, which are considered less reliable than U-Pb and $^{40}Ar/^{39}Ar$ ages, and (3) the unjustified assumption of equal duration of biochronologic units is used for interpolation and the estimation of boundary ages. Recent integrated dating around the critical extinction intervals, primarily using U-Pb geochronology and ammonite biochronology from the western North American Cordillera, is summarized here. This work led to the first interpolation-free, independent stage and zonal boundary and duration estimates (Pálfy et al. 2000b; Fig. 1). The biochronological underpinning of the time scale is a North American regional ammonoid zonal scheme correlated with the primary standard chronostratigraphy of northwestern Europe (Smith et al., 1988, 1994; Jakobs et al., 1994).

Age of the end-Triassic event

It is generally accepted that a mass extinction corresponds to the Triassic-Jurassic (Tr-J) system boundary, even though detailed documentation is hindered by a dearth of fossiliferous and continuous sections worldwide (Hallam, 1990). One of the four proposed sections for the basal Jurassic Global Stratotype Section and Point is located on Kunga Island (Queen Charlotte Islands, British Columbia). At this locality, a tuff layer in the marine sedimentary section that contains the Tr-J boundary yielded a U-Pb zircon age of 199.6 $\pm$ 0.4 Ma (Pálfy et al., 2000a). This age provides a direct estimate for the age of the Tr-J boundary because the sampled layer is immediately below the system boundary as defined by integrated radiolarian, ammonoid, and conodont biochronology. Ages quoted by published time scales are invariably older by several million years (Fig. 1). The two most widely used estimates are 208.0 $\pm$ 7.5 Ma (Harland et al., 1990) and 205.7 $\pm$ 4.0 Ma (Gradstein et al., 1994). Other time scales list 208 Ma (Palmer, 1983), 210 Ma (Haq et al., 1988), and 203 Ma (Odin, 1994) as the best boundary estimates. Several additional biostratigraphically defined U-Pb dates were recently obtained from marine island arc terranes of the North American Cordillera (Table 1). These dates were not considered in previous time scales, but they convincingly support the conclusion that the true age of the Tr-J boundary is close to 200 Ma (Pálfy et al., 2000a).

The age of the end-Triassic extinction can also be estimated from terrestrial sections in eastern North America, where precise U-Pb dates are available from volcanic units within the continental Newark Supergroup (Dunning and Hodych, 1990; Hodych and Dunning, 1992). The North Mountain Basalt was dated as 201.7 $+$ 1.4/$-$1.1 Ma, whereas the Palisades and Gettysburg sills yielded ages of 200.9 $\pm$ 1.0 Ma and 201.3 $\pm$ 1.0 Ma, respectively. On the basis of geochemical and field evidence, the Palisades sill appears to have fed the lowermost flows of the Orange Mountain Basalt (Ratcliffe, 1988). The extrusive volcanic rocks postdate the palynologically defined Tr-J boundary (Fowell and Olsen, 1993) by only 20–40 k.y., on the basis of cyclostratigraphic evidence (Olsen et al., 1996). Vertebrate extinction, as deduced from tetrapod remains (Olsen et al., 1987) and their trace fossil record (Silvestri and Szajna, 1993), is coincident with the peak in floral turnover. The three overlapping isotopic ages and their respective errors suggest that the terrestrial extinction occurred no later than 200.6 Ma. The marine event, best represented by a sharp turnover in radiolarian taxa and delimited by the U-Pb age from Kunga Island, did not occur before 200.0 Ma. Taking these dates at face value suggests that the crisis of terrestrial biota preceded that of the marine realm by at least 600 k.y. (Pálfy et al., 2000a). This is the first indication of such temporal dichotomy within a major mass extinction.

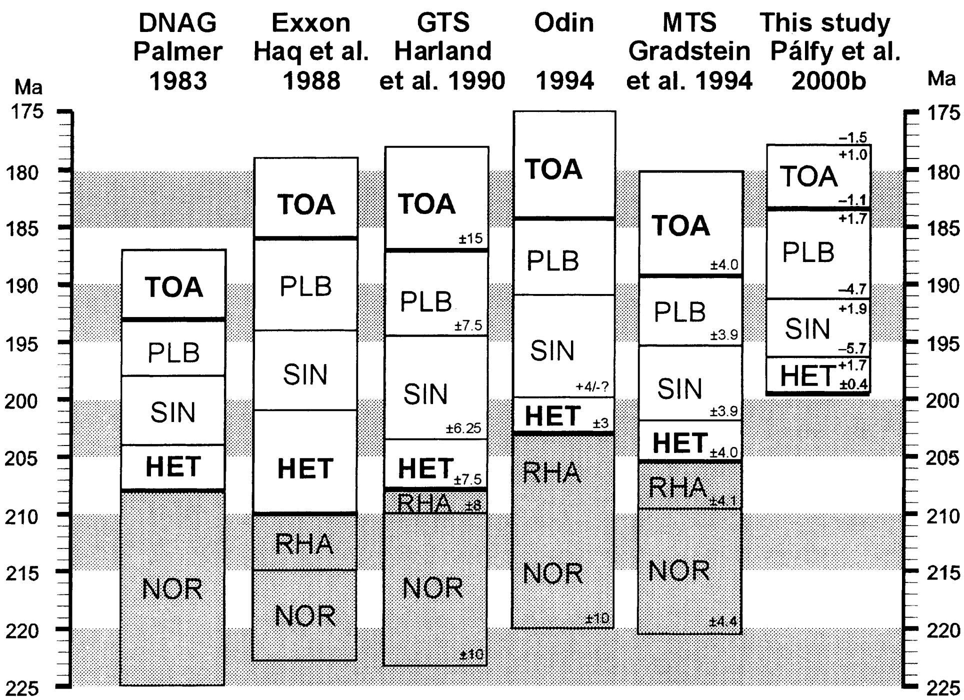

Figure 1. Comparison of Early Jurassic and latest Triassic (shaded) numerical time scales. Note different estimates for age of Triassic-Jurassic and Pliensbachian-Toarcian boundaries in previously widely used time scales vs. revised scale of Pálfy et al. (2000b). Small numbers at stage boundaries indicate stated uncertainty of estimates. Stage abbreviations: NOR, Norian; RHA, Rhaetian; HET, Hettangian; SIN, Sinemurian; PLB, Pliensbachian; TOA, Toarcian. Time-scale abbreviations: DNAG, Decade of North American Geology; GTS, geological time scale; MTS, Mesozoic time scale. Note that Rhaetian stage is not recognized by DNAG scale, whereas Odin (1994) did not estimate age of Norian-Rhaetian boundary.

TABLE 1. LIST OF RECENTLY PUBLISHED U-Pb ZIRCON DATES RELEVANT TO THE AGE OF THE TRIASSIC-JURASSIC BOUNDARY

Dated rock	Locality	U-Pb age (Ma)	Biochronologic age: Maximum	Biochronologic age: Minimum
Tuff in Talkeetna Formation	Puale Bay, Alaska	197.8 ± 1.0	Middle Hettangian	Late Hettangian
Tuff in Talkeetna Formation	Puale Bay, Alaska	197.8 ± 1.2/ – 0.4	Middle Hettangian	Late Hettangian
Tuff in Kamishak Formation	Puale Bay, Alaska	200.8 ± 2.8	Middle Hettangian	Middle Hettangian
Goldslide Porphyry (Goldslide Intrusions)	Stewart, B.C.	197.6 ± 1.9	Hettangian	Hettangian
Tuff in Hazelton Group	Stewart, B.C	199 ± 2	Hettangian	Hettangian
Biotite Porphyry (Goldslide Intrusions)	Stewart, B.C	201.8 ± 0.5	Norian	Rhaetian
Griffith Creek volcanics	Spatsizi River, British Columbia	205.8 ± 0.9	Norian	Rhaetian
Griffith Creek volcanics	Spatsizi River, British Columbia	205.8 ± 1.5/ – 3.1	Norian	Rhaetian

Note: References to sources of isotopic ages and their biochronologic constraints are given in Pálfy et al. (2000b). See Figure 1 for stages.

Age of the Early Jurassic event

An Early Jurassic (Pliensbachian) extinction event was first recognized from a global database of the stratigraphic ranges of marine animal families and genera resolved to stratigraphic stages (Raup and Sepkoski, 1984). An independent compilation of fossil families detected to 5% marine extinction in both the Pliensbachian and Toarcian, and 2.4%–12.8% extinction among continental organisms in the Toarcian (Benton, 1995). On the basis of detailed analysis of the fossil record of northwestern European epicontinental seas, Hallam (1986, 1996a) regarded the extinction as a regional event (Fig. 2D), the later phase of which coincided with widespread anoxia in the early Toarcian Falciferum zone (Jenkyns, 1988). Little and Benton (1995) analyzed the time distribution of global family extinctions and found that a protracted interval of five zones spanning the Pliensbachian-Toarcian stage boundary showed elevated extinction levels (Fig. 2C). However, outcrop-scale studies of the most fossiliferous sections in England and Germany displayed a clear species extinction peak correlating with the anoxic event in the Falciferum zone (Little, 1996). The global extent of the Pliensbachian-Toarcian extinction event was established through detailed studies in the Andean basin (Aberhan and Fürsich, 1997) and deep-water facies of the western Tethys (Vörö, 1993) and Japan (Hori, 1993).

Previous best estimates for the Pliensbachian-Toarcian boundary are 187.0 ± 15 Ma (Harland et al., 1990) and 189.6 ± 4.0 (Gradstein et al., 1994). This portion of our revised Jurassic time scale is built upon 14 recently obtained U-Pb ages from volcanic layers that are also dated by ammonoid biochronology in the North American Cordillera (Pálfy et al., 2000b). None of these isotopic ages had been used in earlier

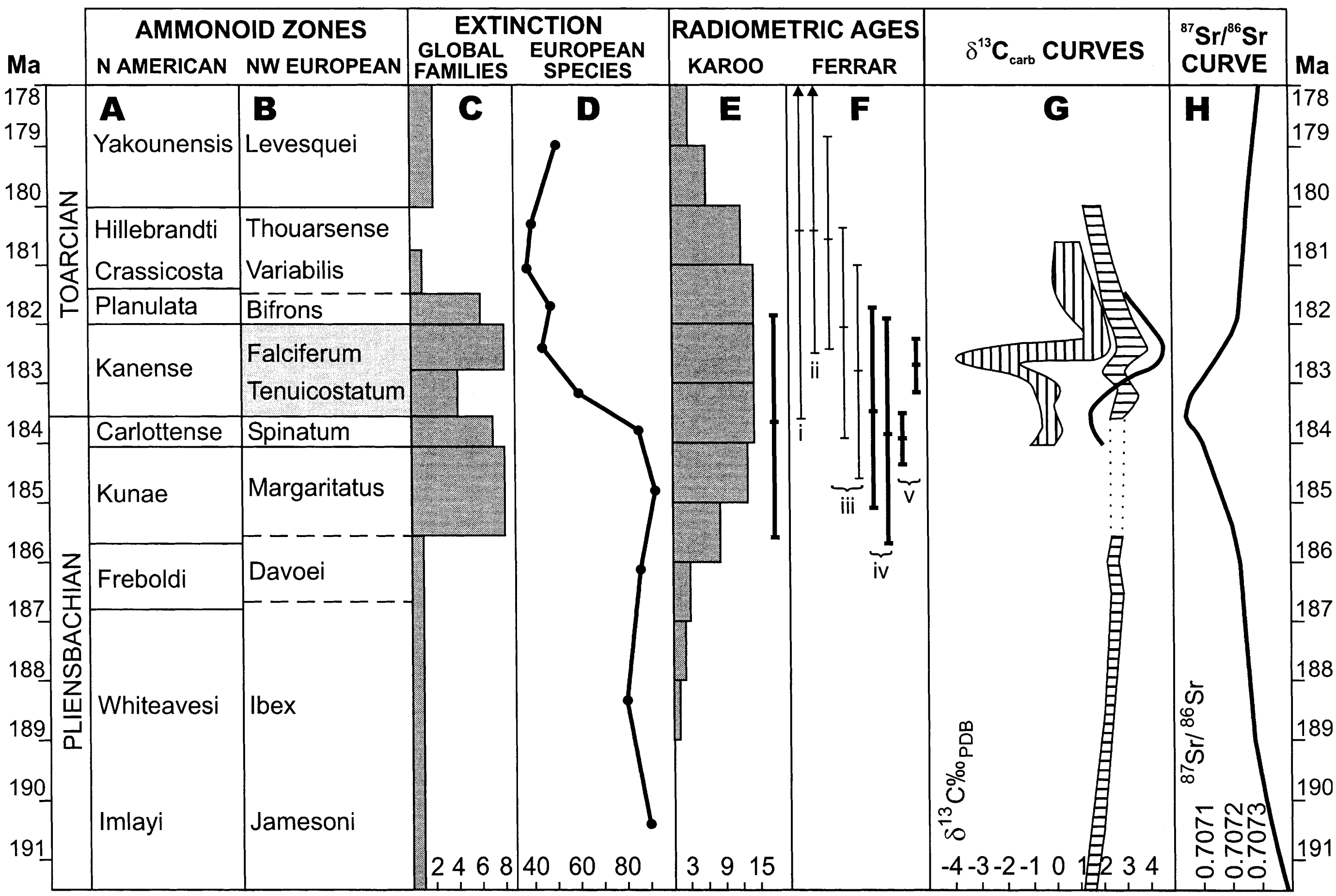

Figure 2. Correlation of marine extinction event, Karoo and Ferrar flood basalt volcanism, and carbon and strontium isotope stratigraphy in numerically calibrated ammonoid zonal chronostratigraphic framework. A: North American regional standard ammonoid zonation (Pliensbachian: Smith et al., 1988; Toarcian: Jakobs et al., 1994); lack of horizontal line between zones indicates that no numerical estimate is available for zone boundary. B: Northwest European standard ammonoid zonation; shading indicates extent of organic-rich deposits in Tenuicostatum and Falciferum zones in western Tethys and northwest Europe. C: Number of global family extinctions by zone (Little and Benton, 1995). D: Cumulative species diversity per zone, expressed in number of species of bivalves, ammonoids, rhynchonellid brachiopods, crinoids, foraminifera, and ostracods from Britain (Hallam, 1996a). E: Radiometric ages from Karoo Group (recalculated from published sources with corrected standard ages for $^{40}Ar/^{39}Ar$ geochronology and 2σ external errors [unless indicated otherwise] for valid comparison; Renne et al., 1998); age spectrum histogram of 28 $^{40}Ar/^{39}Ar$ dates with 1σ internal errors (Duncan et al., 1997); and error bar of U-Pb age (Encarnación et al., 1996). F: $^{40}Ar/^{39}Ar$ (thin lines) and U-Pb (heavy lines) ages from Ferrar Group (recalculated from published sources with corrected standard ages for $^{40}Ar/^{39}Ar$ geochronology and 2σ external errors for valid comparison; Renne et al., 1998). Error bars, from left to right: I, composite of 11 $^{40}Ar/^{39}Ar$ ages by Heimann et al. (1994); ii, composite of two $^{40}Ar/^{39}Ar$ ages by Foland et al. (1993); iii, three $^{40}Ar/^{39}Ar$ ages by Duncan et al. (1997); iv, two U-Pb ages by Encarnación et al. (1996); and v, two U-Pb ages by Minor and Mukasa (1997). G: Carbon isotope profiles: horizontal hachure, composite profile from Central Apennines, Italy (E. Morettini, 1999, personal commun.); vertical hachure, England (Jenkyns and Clayton, 1997; Hesselbo et al., 2000); solid line, composite curve from Tethyan sections (Jenkyns et al., 1991). H: Seawater $^{87}Sr/^{86}Sr$ curve simplified from Jones et al. (1994); monotonous decline of curve starts in Hettangian from values >0.7077 (modified from Pálfy and Smith, 2000).

time scales (Table 2). The density and biochronologic resolution of the isotopic age database across the Pliensbachian-Toarcian transition allows, for the first time, the estimation of zonal boundary ages for six consecutive zones. Zonal boundary ages are calculated using the chronogram method (Harland et al., 1990), except for the base of Crassicosta zone, which is directly dated in the Queen Charlotte Islands (Pálfy et al., 1997). Ammonoid provinciality warrants the use of the North American regional ammonoid zonal scale (Fig. 2A), which is correlated with the northwest European standard chronostratigraphy following Smith et al. (1988) and Jakobs et al. (1994) (Fig. 2B). Calculated best estimates for initial zonal boundaries are as follows (Fig. 2A): Kunae zone (early-late Pliensbachian boundary), 185.7 + 0.5/ −0.6 Ma; Carlottense zone: 184.1 + 1.2/−1.6 Ma; Kanense zone (Pliensbachian-Toarcian boundary), 183.6 + 1.7/−1.1 Ma; Planulata zone, 182.0 + 3.3/−1.8 Ma; Crassicosta zone, 181.4 ± 1.2 Ma.

TABLE 2. LIST OF RECENTLY PUBLISHED U-Pb ZIRCON DATES USED IN ESTIMATING THE AGE OF PLIENSBACHIAN AND TOARCIAN ZONAL BOUNDARIES

Dated rock	Locality	U-Pb age (Ma)	Biochronologic age (zone or stage)	
			Maximum	Minimum
Chuchi intrusion	Chuchi property	188.5 ± 2.5	Whiteavesi	Kunae
Tuff in Laberge Group	Atlin Lake (East shore)	187.5 ± 1.0	Whiteavesi	Whiteavesi
Tuff in Hazelton Group	Todagin Mountain, Spatsizi area	185.6 ± 7.3/−0.6	Freboldi	Freboldi
Granitoid boulder in Laberge Gr.	Atlin Lake (Sloko Island)	186.6 ± 0.5/−1.0*	Sinemurian	Kunae
Tuff in Laberge Group	Atlin Lake (Copper Island)	185.8 ± 0.7	Kunae	Kunae
Tuff in Hazelton Group	Skinhead Lake	184.7 ± 0.9	Kunae	Kunae
Tuff (Nordenskiold volcanics)	Whitehorse	184.1 ± 5.8/−1.6	Kunae	Kunae
Eskay porphyry	Eskay Creek, Iskut River area	184 ± 6/−1	Carlottense	Aalenian
McEwan Creek pluton	McEwan Creek, Spatsizi area	183.2 ± 0.7	Kanense	Planulata
Tuff in Hazelton Group	Mt. Brock range, Spatsizi area	180.4 ± 11.2/−0.4	Kanense	Planulata
Tuff in Whiteaves Formation	Yakoun River, Queen Charlotte Island	181.4 ± 1.2	Crassicosta	Crassicosta
Tuff in Hazelton Group	Julian Lake	178 ± 1	Yakounensis	Aalenian
Eskay rhyolite	Eskay Creek anticline, west limb	175.1 ± 4.7	Yakounensis	Aalenian
Eskay rhyolite	Eskay Creek anticline, east limb	174.1 ± 4.5/−1.1	Yakounensis	Aalenian

*Maximum age.
References to sources of isotopic ages and their biochronologic constraints are given in Pálfy et al. (2000b).
See Figure 2 for ammonoid zones.

RADIOMETRIC DATING OF COEVAL VOLCANIC EVENTS

The flood basalt volcanism of large igneous provinces has been invoked as a cause of extinctions (e.g., Rampino and Stothers, 1988, Courtillot, 1994). Although the proposal was made on broad time correlation when the numerical ages of both the volcanic provinces and the extinction boundaries were poorly established, recent advances permit a reevaluation of temporal linkages.

Age of the Central Atlantic magmatic province

Basalts around the margins of the central Atlantic form a vast, once contiguous volcanic province, termed the Central Atlantic magmatic province. The volume of coeval volcanic rocks is estimated to be in excess of 2×10^6 km^3 (Marzoli et al., 1999); thus the Central Atlantic magmatic province ranks among the most voluminous of the Phanerozoic volcanic provinces. Tholeiitic basalts of the Central Atlantic magmatic province are now exposed along the eastern seaboard of North America, Brazil, and adjacent parts of northeastern South America, western Africa, and the Iberian Peninsula.

Recent studies significantly improved the dating of this extensive basaltic volcanism. The ^{40}Ar/^{39}Ar dating by Marzoli et al. (1999), mainly from previously undated areas in South America, documented that Central Atlantic magmatic province eruptions represent a short-lived episode that reached its peak intensity at 200 Ma. Marzoli et al. compiled a total of 41 newly reported and previously published ^{40}Ar/^{39}Ar and U-Pb dates, and calculated a mean age of 199.0 ± 2.4 Ma (2σ external error). This data set includes U-Pb dates from the Newark Supergroup discussed herein. Further ^{40}Ar/^{39}Ar dating of related rocks from the southwestern United States is fully compatible with this age distribution (Hames et al., 2000).

An additional line of evidence for a short-lived volcanic pulse is furnished by paleomagnetic studies. Kent et al. (1995) documented that extrusive rocks in the Newark Supergroup all belong to the single normal polarity chron that spans the Tr-J boundary. Similarly, paleomagnetic data from South American reported by Marzoli et al. (1999) and previous studies summarized therein all revealed normal magnetic polarity for Central Atlantic magmatic province volcanic rocks.

Age of the Karoo-Ferrar volcanic province

The Karoo province in South Africa and the Ferrar province in Antarctica are disjunct parts of a once contiguous large igneous province of Jurassic age in Gondwana. The estimated minimum volume of coeval igneous rocks is 2.5×10^6 km^3 (Encarnación et al., 1996); thus it ranks among the most voluminous flood basalt provinces of the Phanerozoic (Rampino and Stothers, 1988). Early radiometric dating, relying on the K-Ar method, was plagued with problems. A suite of whole-rock ages for the Karoo Group is distributed between 135 and 225 Ma, with apparent peaks of volcanic intensity at 193 ± 5 and 178 ± 5 Ma (Fitch and Miller, 1984). The K-Ar chronometer often yields anomalously young or old ages in disturbed systems, due to Ar loss or uptake of excess Ar, respectively. The use of ^{40}Ar/^{39}Ar and U-Pb dating, however, permits reliable determination of the true crystallization age of mafic igneous rocks. For valid comparison between dates recently obtained using different isotopic methods, we recalculated the published ages to reflect external errors (i.e., including decay constant uncertainty) at the 2σ level and the currently accepted ages of standards for ^{40}Ar/^{39}Ar dating (Renne et al., 1998).

Duncan et al. (1997) reported 28 precise ^{40}Ar/^{39}Ar plateau ages from Karoo Group basalts and dolerites in South Africa and Namibia. The ages range between 179 and 186 Ma, with a majority at 183 $\pm$ 2 Ma (Fig. 2E). A U-Pb age of 183.7 $\pm$ 1.9 Ma obtained by Encarnación et al. (1996) from a tholeiitic sheet in South Africa is in good agreement with the $^{40}Ar/^{39}Ar$ results (Fig. 2E).

Various units within the Ferrar Group in Antarctica have also been dated (Fig. 2F). From the Kirkpatrick Basalt, Foland et al. (1993) reported two nearly identical incremental heating $^{40}Ar/^{39}Ar$ ages of 180.4 $\pm$ 2.1 Ma. Also from the Kirkpatrick Basalt, Heimann et al. (1994) reported 11 $^{40}Ar/^{39}Ar$ plateau ages that form a tight cluster and permit a composite age determination of 180.3 $\pm$ 3.6 Ma. Basalts from the Kirwan Mountains, East Antarctica, yielded $^{40}Ar/^{39}Ar$ plateau ages of 180.6 $\pm$ 1.8, 182.7 $\pm$ 1.8, and 182.8 $\pm$ 1.8 Ma (Duncan et al., 1997). Concordant U-Pb ages of 183.4 $\pm$ 1.9 and 183.8 $\pm$ 1.9 were obtained by Encarnación et al. (1996) from sills within the Ferrar Group. Minor and Mukasa (1997) dated (U-Pb) two samples from the Dufek intrusion (which forms part of the Ferrar Group) as 183.9 $\pm$ 0.4 and 182.7 $\pm$ 0.5 Ma.

These radiometric ages suggest a short-lived magmatic episode, represented by coeval rocks of the Karoo and Ferrar Groups. Such brevity of volcanism is typical of most other large flood basalt provinces of the world (Coffin and Eldholm, 1994). The cluster of ages around 183 $\pm$ 2 Ma is interpreted as the peak of magmatic activity. Additional support for a short-lived magmatic episode is provided by paleomagnetic results. Hargraves et al. (1997) demonstrated that the bulk of basalts in the Karoo province erupted during a single polarity epoch.

INTERVAL BETWEEN EXTINCTIONS

Ever since the Cretaceous-Tertiary extinction was first linked to an extraterrestrial impact (Alvarez et al., 1980), other mass extinction horizons have been scrutinized for impact signatures. The case has also been made that extraterrestrial impacts were the prime causes of many or all extinctions based, in part, on their periodicity and the well-established Cretaceous-Tertiary case of synchrony (Raup and Sepkoski, 1984; Rampino and Haggerty, 1996). The end-Triassic and the Toarcian events represent two consecutive mass extinctions in a series of such events that were hypothesized to exhibit periodicity at a 26 m.y. phase length (Raup and Sepkoski, 1984). The periodicity hypothesis has been much debated and one frequently cited argument against it is the deficiency of the underlying time scale (Hoffman, 1985; Heisler and Tremaine, 1989). When updating the extinction time series analysis using the Harland et al. (1990) time scale, Sepkoski (1996) found that the end-Triassic and Pliensbachian extinctions did not closely follow the 26 m.y. pattern.

A corollary of our refined dating is a fresh look at the spacing of mass extinctions in question. The revised time scale confirms that the spacing of these two events is significantly less than 26 m.y. Accepting 199.6 $\pm$ 0.4 Ma as the best estimate for the Triassic-Jurassic boundary and 182.0 $+3.3/-1.8$ Ma as the end of the Falciferum zone, i.e., a time that postdates the Toarcian species extinction peak, it is evident that the two consecutive extinction events likely took place less than 18 m.y. apart.

ISOTOPIC EVIDENCE FOR SYNCHRONOUS GLOBAL ENVIRONMENTAL PERTURBATIONS

Stable isotope stratigraphy is a powerful tool for reconstructing past environmental change. Dramatic environmental changes, accompanied by disruption and reorganization of the global carbon cycle and other biogeochemical cycles, are known to occur associated with mass extinctions. There is ample evidence for pronounced isotopic excursions associated with many extinction events, most notably the end-Permian and the end-Cretaceous events (e.g., Baud et al., 1989; Zachos et al., 1989; Holser et al., 1996). Carbon isotope stratigraphy is especially useful for documenting changes in the biogeochemical cycling of carbon (Kump and Arthur, 1999), whereas oxygen isotopes are widely used for paleotemperature reconstruction. In addition, strontium isotope stratigraphy can be used as a proxy for changes in paleoclimate and global tectonics (e.g., Hodell and Woodruff, 1994).

Having established the temporal synchrony between early Mesozoic pulses of flood basalt volcanism and extinctions, isotopic signatures may provide clues to their cause and effect relationship.

Stable isotope record across the Tr-J boundary

Until recently, relatively little was known about the stable isotope history of the end-Triassic event. Among the available marine sections, early work concentrated on Kendelbachgraben (Morante and Hallam, 1996) and Lorüns (McRoberts et al., 1997) in Austria and New York Canyon in Nevada (Taylor et al., 1992). All met with mixed success. McRoberts et al. (1997) reported a small negative anomaly confined to a single sample from the boundary interval in the Lorüns section. However, at this locality the boundary is defined by bivalves; hence the stratigraphic completeness of the section cannot be proven. At Kendelbachgraben, a negative $\delta^{13}C_{carb}$ excursion is accompanied by a positive $\delta^{13}C_{org}$ and a negative $\delta^{18}O$ excursion, indicating diagenetic overprint rather than a primary signal (Hallam and Goodfellow, 1990; Morante and Hallam, 1996). The preliminary report of isotopic variations from Nevada (Taylor et al., 1992) cannot be properly evaluated. However, significant negative carbon isotope excursions were recently reported from marine Triassic-Jurassic boundary strata of widely separated localities of the eastern Pacific and western Tethys. In the Queen Charlotte Islands, western Canada, a negative $\delta^{13}C$ spike of $-1.5‰$ measured in bulk organic matter, from a level that corresponds to the radiolarian extinction (Ward et al., 2001). An even larger anomaly of up to $-3.5‰$ was detected in both bulk carbonate and organic matter in a section at Csövár, Hungary (Pálfy et al., 2001), within the Triassic-Jurassic transition defined by ammonoid and conodont biostratigraphy. Organic carbon isotopic data from a terrestrial section in Greenland also hint at a negative excursion at the boundary (McElwain et al., 1999).

The available data suggest that the terminal Triassic extinction coincided with a negative carbon isotope anomaly, similar to many other extinction events. However, more research is needed to assess the magnitude and duration of the anomaly, and to interpret the underlying changes in the global carbon cycle.

Stable isotope record of the Toarcian

Recognition of a prominent positive $\delta^{13}C$ excursion in the Falciferum zone, along with widespread organic-rich facies, is the basis for defining an early Toarcian oceanic anoxic event (Jenkyns, 1988). Originally the $\delta^{13}C$ maximum was thought to be restricted to the Falciferum zone, but in several Tethyan sections, the rise of $\delta^{13}C$ begins in the Tenuicostatum zone (Jenkyns et al., 1991; Jiménez et al., 1996; E. Morettini, 1999, personal commun.) (Fig. 2G). Organic-rich black shale deposition is also known in the Tenuicostatum zone in Spain and Italy (Jiménez et al., 1996; E. Morettini, 1999, personal commun.), and manganese-rich deposits are widespread in the Tenuicostatum to Falciferum zones (Jenkyns et al., 1991).

More recent stable isotope results of Hesselbo et al. (2000) indicate that the positive carbon isotope excursion was preceded by a short and intense negative anomaly that is equally measurable in both marine carbonate and terrestrial organic matter. Hesselbo et al. suggested that the isotopically light carbon could have entered the world ocean, the atmosphere, and the biosphere through sudden release of methane hydrate, which in turn might have been triggered by the warming of deep ocean water. The short-lived negative spike needs further investigation, because it has not been confirmed by a study on closely sampled belemnites (McArthur et al., 2000).

A $\delta^{18}O$ minimum in the Falciferum zone records a paleotemperature maximum for the Toarcian (Jenkyns and Clayton, 1997). Jenkyns and Clayton speculated that a correlation with increased CO_2 level is a strong possibility supported by the low $\delta^{13}C$ values of organic matter. The CO_2 from voluminous volcanic outgassing is a possible cause of greenhouse warming that may have been accelerated by gas-hydrate release.

Strontium isotope stratigraphy across the Tr-J boundary

The strontium isotopic evolution across the Tr-J transition is revealed by recent detailed studies from both the Jurassic (Jones et al., 1994) and the Triassic (Korte, 1999). A Late Triassic climb of the $^{87}Sr/^{86}Sr$ ratio was sharply reversed immediately prior to the Tr-J boundary (Veizer et al., 1999). The most likely event that affected the Sr isotopic composition of seawater is the initiation of volcanism in the Central Atlantic Magmatic Province, which could have simultaneously altered the global climate and the composition of exposed rocks.

Strontium isotope stratigraphy of the Pliensbachian-Toarcian

Temporal variations in the $^{87}Sr/^{86}Sr$ ratio of the Early Jurassic oceans were documented by Jones et al. (1994) (Fig. 2H) and refined by McArthur et al. (2000). Following a nearly continuous decline from the Hettangian to the Pliensbachian, the curve reaches a minimum at the Pliensbachian-Toarcian boundary and rises in the Toarcian; the steepest slope is recorded for the Falciferum zone. It is notable that the major Early Jurassic inflection appears to coincide with the inception of Karoo-Ferrar volcanism. The early Toarcian rise can be related to increased humidity and continental weathering, possibly enhanced by acid rain, under escalating greenhouse conditions triggered by volcanic emissions.

DISCUSSION

The synchrony of the end-Triassic extinction and volcanism in the Central Atlantic magmatic province, and the Early Jurassic extinction and volcanism in the Karoo-Ferrar province now appear well established. Geochemical data, primarily carbon and strontium isotope stratigraphy, support models that call on environmental perturbations triggered by volcanism as a potential factor in the biotic extinctions.

Here we discuss three key issues: extinction dynamics, carbon isotope evolution, and strontium isotope evolution. We compare the two extinctions to provide insight and to indicate where further research is most needed.

For the Early Jurassic event, the tempo of extinction was found curiously different at the species level from that at higher taxonomic ranks. Little and Benton (1995) documented that elevated family extinction level was sustained through five zones in the late Pliensbachian-early Toarcian, an interval of 4 m.y. in the revised time scale used here. However, abrupt species-level extinctions are concentrated in the early Toarcian Tenuicostatum zone. The subsequent Falciferum zone can be described as a survival interval, which in turn was followed by rapid repopulation and recovery (Harries and Little, 1999). Thus the Pliensbachian-Toarcian extinction exhibits the attributes of both press and pulse events (Erwin, 1998).

Few similarly detailed studies are available from the Tr-J boundary. Sudden extinction and major turnover are recorded among radiolarians (Carter, 1994), pollen (Fowell and Olsen, 1993), and megaflora (McElwain et al., 1999). The duration of the Rhaetian, a time of protracted decline for many fossil groups including the ammonites, bivalves, and conodonts (Hallam, 1996a), is poorly defined due to a lack of isotopic ages (see Fig. 1). Timing of the earliest Jurassic marine biotic recovery is better known. The early Hettangian (Planorbis zone) is characterized by a low-diversity fauna worldwide and is perhaps best regarded as a postextinction lag or survival period. True recovery and diversification started in the middle Hettangian within many clades (Hallam, 1996b). Hettangian U-Pb dates from Alaska (Table 1) (Pálfy et al., 1999) indicate that recovery was underway within less than 2 m.y. Whether the apparent length of the biotic crisis and the delayed rebound are artifacts of inadequate sampling (Signor and Lipps, 1982; Erwin, 1998) remains to be tested. Attributes of a mixed press and pulse event similar to the Toarcian are apparent from the available data. This pattern and the suggested temporal difference between terrestrial and marine events are consistent with extinction scenarios that invoke long-term environmental change, but with a shorter response time or lower threshold in the more vulnerable terrestrial biota.

Gradual global warming, induced by flood basalt volcanism, may trigger the sudden release of methane hydrate and a positive feedback mechanism that in turn may cause catastrophic climate change and extinctions. This is the scenario suggested by the sharp negative $\delta^{13}C$ spike for the early Toarcian (Hesselbo et al., 2000). Methane hydrate release, first invoked to account for the late Paleocene thermal maximum (Dickens et al., 1995), has also been considered for the Permian-Triassic event (Erwin, 1993; Krull and Retallack, 2000). However, it is not clear whether this model can be applied to the Tr-J extinction event. The need to improve our understanding of the carbon isotope record is underscored by three lines of evidence that suggest that the model may be applicable: (1) paleobotanical data indicate a supergreenhouse Earth at the Tr-J boundary (McElwain et al., 1999), (2) the similar press and pulse dynamics of the two extinction events, and (3) the synchronous occurrence of flood basalt volcanism and extinction.

We suggest that the end-Pliensbachian reversal and Toarcian increase of the Sr isotope ratio records the onset of Karoo-Ferrar volcanism. A similar inflection occurs in the Late Permian, although it appears to slightly predate the Siberian Traps (Martin and Macdougall, 1995). The formation of the Central Atlantic magmatic province around the Tr-J boundary coincides with a downturn of the Sr curve. Modeling suggests that continental flood basalt volcanism could alter seawater chemistry via enhanced weathering and increased riverine flux (Martin and Macdougall, 1995). We speculate that changes of opposite sense across the Tr-J boundary may reflect the low to middle paleolatitude of the Central Atlantic magmatic province (vs. the middle- to high-latitude Siberian Traps and Karoo-Ferrar provinces), whereby basalt weathering exerts greater influence on the oceanic Sr budget and explains a shift toward less radiogenic values (Taylor and Lasaga, 1999).

Advances in our understanding of the early Mesozoic extinctions are expected from further integrated paleontological and geochemical studies. We cannot escape a conclusion that flood basalt volcanism in the Central Atlantic magmatic province and the Karoo-Ferrar provinces likely played a significant role in driving the end-Triassic and Toarcian extinctions, although details of the links are only beginning to emerge.

ACKNOWLEDGMENTS

Pálfy acknowledges support from the Hungarian Scientific Research Fund (grant F23451) and the Alexander von Humboldt Foundation. Presentation of this paper at the Vienna conference was made possible by a grant-in-aid to Pálfy. Smith and Mortenesen acknowledge support of the Natural Sciences and Engineering Research Council of Canada. Reviews and comments by M. Coffin, K. MacLeod, and P.B. Wignall helped improve the manuscript.

REFERENCES CITED

Aberhan, M., and Fürsich, F.T., 1997, Diversity analysis of Lower Jurassic bivalves of the Andean Basin and the Pliensbachian-Toarcian mass extinction: Lethaia, v. 29, p. 181–195.

Alvarez, L., Alvarez, W., Asaro, F., and Michel, H., 1980, Extraterrestrial cause for the Cretaceous-Tertiary extinction: Science, v. 208, p. 1095–1108.

Baud, A., Magaritz, M., and Holser, W.T., 1989, Permian-Triassic of the Tethys: Carbon isotope studies: Geologische Rundschau, v. 78, p. 649–677.

Benton, M.J., 1995, Diversification and extinction in the history of life: Science, v. 268, p. 52–58.

Carter, E.S., 1994, Evolutionary trends in latest Norian through Hettangian radiolarians from the Queen Charlotte Islands, British Columbia: Géobios, Mémoire Spécial, v. 17, p. 111–119.

Coffin, M.F., and Eldholm, O., 1994, Large igneous provinces: Crustal structure, dimensions and external consequences: Reviews of Geophysics, v. 32, p. 1–36.

Courtillot, V., 1994, Mass extinctions in the last 300 million years: One impact and seven flood basalts?: Israel Journal of Earth Sciences, v. 43, p. 255–266.

Dickens, R.G., O'Neil, J.R., Rea, D.K., and Owen, R.M., 1995, Dissociation of oceanic methane hydrate as a cause of the carbon isotope excursion at the end of the Paleocene: Paleoceanography, v. 10, p. 965–971.

Duncan, R.A., Hooper, P.R., Rehacek, J., Marsh, J.S., and Duncan, A.R., 1997, The timing and duration of the Karoo igneous event, southern Gondwana: Journal of Geophysical Research, v. 102, p. 18127–18138.

Dunning, G.R., and Hodych, J.P., 1990, U/Pb zircon and baddeleyite ages for the Palisades and Gettysburg sills of the northeastern United States: Implications for the age of the Triassic/Jurassic boundary: Geology, v. 18, p. 795–798.

Encarnación, J., Fleming, T.H., Elliot, D.H., and Eales, H., 1996, Synchronous emplacement of Ferrar and Karoo dolerites and the early breakup of Gondwana: Geology, v. 24, p. 535–538.

Erwin, D.H., 1993, The great Paleozoic crisis: New York, Columbia University Press, 327 p.

Erwin, D.H., 1998, The end and the beginning: Recoveries from mass extinctions: Trends in Ecology & Evolution, v. 13, p. 344–349.

Fitch, F.J., and Miller, J.A., 1984, Dating Karoo igneous rocks by the conventional K/Ar and $^{40}Ar/^{39}Ar$ age spectrum methods, *in* Erlank, A.J., ed., Petrogenesis of the volcanic rocks of the Karoo Province: Geological Society of Africa Special Publication 13, p. 247–266.

Foland, K.A., Fleming, T.H., Heimann, A., and Elliot, D.H., 1993, Potassium-argon dating of fine-grained basalts with massive Ar-loss: Application of the $^{40}Ar/^{39}Ar$ technique to plagioclase and glass from the Kirkpatrick Basalt, Antarctica: Chemical Geology, v. 107, p. 173–190.

Fowell, S.J., and Olsen, P.E., 1993, Time calibration of Triassic/Jurassic microfloral turnover, eastern North America: Tectonophysics, v. 222, p. 361–369.

Gradstein, F.M., Agterberg, F.P., Ogg, J.G., Hardenbol, J., van Veen, P., Thierry, J., and Huang, Z., 1994, A Mesozoic time scale: Journal of Geophysical Research, v. 99, p. 24051–24074.

Hallam, A., 1986, The Pliensbachian and Tithonian extinction events: Nature, v. 319, p. 765–768.

Hallam, A., 1990, The end-Triassic mass extinction event, *in* Sharpton, V.L., and Ward, P.D., eds., Global catastrophes in Earth history: An interdisciplinary conference on impacts, volcanism, and mass mortality: Geological Society of America Special Paper 247, p. 577–583.

Hallam, A., 1996a, Major bio-events in the Triassic and Jurassic, *in* Walliser, O.H., ed., Global events and event stratigraphy in the Phanerozoic: Berlin, Springer-Verlag, p. 265–283.

Hallam, A., 1996b, Recovery of the marine fauna in Europe after the end-Triassic and early Toarcian mass extinctions, *in* Hart, M.B., ed., Biotic recovery from mass extinction events: Geological Society [London] Special Publication 102, p. 231–236.

Hallam, A., and Goodfellow, W.D., 1990, Facies and geochemical evidence bearing on the end-Triassic disappearance of the Alpine reef ecosystem: Historical Biology, v. 4, p. 131–138.

Hames, W.E., Renne, P.R., and Ruppel, C., 2000, New evidence for geologically instantaneous emplacement of earliest Jurassic Central Atlantic Magmatic Province basalts on the North American margin: Geology, v. 28, p. 859–862.

Haq, B.U., Hardenbol, J., and Vail, P.R., 1988, Mesozoic and Cenozoic chronostratigraphy and cycles of sea level change: Society of Economic Paleontologists and Mineralogists Special Publication 42, p. 71–108.

Hargraves, R.B., Rehacek, J., and Hooper, P.R., 1997, Paleomagnetism of the Karoo igneous rocks in South Africa: South African Journal of Geology, v. 100, p. 195–212.

Harland, W.B., Armstrong, R.L., Cox, A.V., Craig, L.E., Smith, A.G., and Smith, D.G., 1990, A geologic time scale 1989: Cambridge, Cambridge University Press, 263 p.

Harries, P.J., and Little, C.T.S., 1999, The early Toarcian (Early Jurassic) and the Cenomanian-Turonian (Late Cretaceous) mass extinctions: Similarities and contrasts: Palaeogeography, Palaeoclimatology, Palaeoecology, v. 154, p. 39–66.

Heimann, A., Fleming, T.H., Elliot, D.H., and Foland, K.A., 1994, A short interval of Jurassic continental flood basalt volcanism in Antarctica as demonstrated by $^{40}Ar/^{39}Ar$ geochronology: Earth and Planetary Science Letters, v. 121, p. 19–41.

Heisler, J., and Tremaine, S., 1989, How dating uncertainties affect the detection of periodicity in extinctions and craters: Icarus, v. 77, p. 213–219.

Hesselbo, S.P., Gröcke, D.R., Jenkyns, H.C., Bjerrum, C.J., Farrimond, P., Morgans Bell, H.S., and Green, O.R., 2000, Massive dissociation of gas hydrate during a Jurassic oceanic anoxic event: Nature, v. 406, p. 392–395.

Hodell, D.A., and Woodruff, F., 1994, Variations in the strontium isotopic ratio of seawater during the Miocene: Stratigraphic and geochemical implications: Paleoceanography, v. 9, p. 405–426.

Hodych, J.P., and Dunning, G.R., 1992, Did the Manicouagan impact trigger end-of-Triassic mass extinction?: Geology, v. 20, p. 51–54.

Hoffman, A., 1985, Patterns of family extinction: Dependence on definition and geologic time scale: Nature, v. 315, p. 659–662.

Holser, W.T., Magaritz, M., and Ripperdan, R.L., 1996, Global isotopic events, *in* Walliser, O.H., ed., Global events and event stratigraphy in the Phanerozoic: Berlin, Springer-Verlag, p. 63–88.

Hori, S.R., 1993, Toarcian oceanic event in deep-sea sediments: Geological Survey of Japan Bulletin, v. 44, p. 555–570.

Jakobs, G.K., Smith, P.L., and Tipper, H.W., 1994, An ammonite zonation for the Toarcian (Lower Jurassic) of the North American Cordillera: Canadian Journal of Earth Sciences, v. 31, p. 919–942.

Jenkyns, H.C., 1988, The early Toarcian (Jurassic) anoxic event: Stratigraphic, sedimentary, and geochemical evidence: American Journal of Science, v. 288, p. 101–151.

Jenkyns, H.C., and Clayton, C., 1997, Lower Jurassic epicontinental carbonates and mudstones from England and Wales: Chemostratigraphic signals and the early Toarcian anoxic event: Sedimentology, v. 44, p. 687–706.

Jenkyns, H.C., Géczy, B., and Marshall, J.D., 1991, Jurassic manganese carbonates of central Europe and the early Toarcian anoxic event: Journal of Geology, v. 99, p. 137–149.

Jiménez, A.P., Jiménez de Cisneros, C., Rivas, P., and Vera, J.A., 1996, The early Toarcian anoxic event in the westernmost Tethys (Subbetic): Paleogeographic and paleobiogeographic significance: Journal of Geology, v. 104, p. 399–416.

Jones, C.E., Jenkyns, H.C., and Hesselbo, S.P., 1994, Strontium isotopes in Early Jurassic seawater: Geochimica et Cosmochimica Acta, v. 58, p. 1285–1301.

Kent, D.V., Olsen, P.E., and Witte, W.K., 1995, Late Triassic-earliest Jurassic geomagnetic polarity sequence and paleolatitudes from drill cores in the Newark rift basin, eastern North America: Journal of Geophysical Research, v. 100, p. 14965–14998.

Korte, C., 1999, $^{87}Sr/^{86}Sr$-, $\delta^{18}O$- und $\delta^{13}C$-evolution des triassischen Meerwassers: geochemische und stratigraphische Untersuchungen an Conodonten und Brachiopoden: Bochumer Geologische und Geotechnische Arbeiten, v. 52, p. 1–171.

Krull, E.S., and Retallack, G.J., 2000, $\delta^{13}C$ depth profiles from paleosols across the Permian-Triassic boundary: Evidence for methane release: Geological Society of America Bulletin, v. 112, p. 1459–1472.

Kump, L.R., and Arthur, M.A., 1999, Interpreting carbon-isotope excursions: Carbonates and organic matter: Chemical Geology, v. 161, p. 181–198.

Little, C.T.S., 1996, The Pliensbachian-Toarcian (Lower Jurassic) extinction event, *in* Ryder, G., et al., eds., The Cretaceous-Tertiary event and other catastrophes in Earth history: Geological Society of America Special Paper 307, p. 505–512.

Little, C.T.S., and Benton, M.J., 1995, Early Jurassic mass extinction: A global long-term event: Geology, v. 23, p. 495–498.

Martin, E.E., and Macdougall, J.D., 1995, Sr and Nd isotopes at the Permian/Triassic boundary: A record of climate change: Chemical Geology, v. 125, p. 73–100.

Marzoli, A., Renne, P.R., Piccirillo, E.M., Ernesto, M., Bellieni, G., and De Min, A., 1999, Extensive 200-million-year-old continental flood basalts of the Central Atlantic Magmatic Province: Science, v. 284, p. 616–618.

McArthur, J.M., Donovan, D.T., Thirlwall, M.F., Fouke, B.W., and Mattey, D., 2000, Strontium isotope profile of the Early Toarcian (Jurassic) Oceanic Anoxic Event, the duration of ammonite biozones, and belemnite paleotemperatures: Earth and Planetary Science Letters, v. 179, p. 269–285.

McElwain, J.C., Beerling, D.J., and Woodward, F.I., 1999, Fossil plants and global warming at the Triassic-Jurassic boundary: Science, v. 285, p. 1386–1390.

McRoberts, C.A., Furrer, H., and Jones, D.S., 1997, Palaeoenvironmental interpretation of a Triassic-Jurassic boundary section from Western Austria based on palaeoecological and geochemical data: Palaeogeography, Palaeoclimatology, Palaeoecology, v. 136, p. 79–95.

Minor, D.R., and Mukasa, S.B., 1997, Zircon U-Pb and hornblende $^{40}Ar/^{39}Ar$ ages for the Dufek layered mafic intrusion, Antarctica: Implications for the age of the Ferrar large igneous province: Geochimica et Cosmochimica Acta, v. 61, p. 2497–2504.

Morante, R., and Hallam, A., 1996, Organic carbon isotopic record across the Triassic-Jurassic boundary in Austria and its bearing on the cause of the mass extinction: Geology, v. 24, no. 5, p. 391–394.

Odin, G.S., 1994, Geological time scale: Comptes Rendus de l'Académie des Sciences, Paris, Série 2, v. 318, p. 59–71.

Olsen, P.E., Schlische, R.W., and Fedosh, M.S., 1996, 580 ky duration of the Early Jurassic flood basalt event in eastern North America estimated using Milankovitch cyclostratigraphy, *in* Morales, M., ed., The continental Jurassic: Museum of Northern Arizona Bulletin 60, p. 11–22.

Olsen, P.E., Shubin, N.H., and Anders, M.H., 1987, New Early Jurassic tetrapod assemblages constrain Triassic-Jurassic tetrapod extinction event: Science, v. 237, p. 1025–1029.

Pálfy, J., Demény, A., Haas, J., Hetényi M., Orchard, M., and Vetö, I., 2001, Carbon isotope anomaly and other geochemical changes at the Triassic-Jurassic boundary from a marine section in Hungary: Geology, v. 29, p. 1047–1050.

Pálfy, J., and Smith, P.L., 2000, Synchrony between Early Jurassic extinction, oceanic anoxic event, and the Karoo-Ferrar flood basalt volcanism: Geology, v. 28, p. 747–750.

Pálfy, J., Parrish, R.R., and Smith, P.L., 1997, A U-Pb age from the Toarcian (Lower Jurassic) and its use for time scale calibration through error analysis of biochronologic dating: Earth and Planetary Science Letters, v. 146, p. 659–675.

Pálfy, J., Smith, P.L., Mortensen, J.K., and Friedman, R.M., 1999, Integrated ammonite biochronology and U-Pb geochronology from a Lower Jurassic section in Alaska: Geological Society of America Bulletin, v. 111, p. 1537–1549.

Pálfy, J., Mortensen, J.K., Carter, E.S., Smith, P.L., Friedman, R.M., and Tipper, H.W., 2000a, Timing the end-Triassic mass extinction: First on land, then in the sea?: Geology, v. 28, p. 39–42.

Pálfy, J., Mortensen, J.K., and Smith, P.L., 2000b, A U-Pb and $^{40}Ar/^{39}Ar$ time scale for the Jurassic: Canadian Journal of Earth Sciences, v. 37, p. 923–944.

Palmer, A.R., 1983, The Decade of North American Geology 1983 geologic time scale: Geology, v. 11, p. 503–504.

Rampino, M.R., and Haggerty, B.M., 1996, Impact crises and mass extinction: A working hypothesis, *in* Ryder, G., et al., eds., The Cretaceous-Tertiary event and other catastrophes in Earth history: Geological Society of America Special Paper 307, p. 11–30.

Rampino, M.R., and Stothers, R.B., 1988, Flood basalt volcanism during the last 250 million years: Science, v. 241, p. 663–667.

Ratcliffe, N.M., 1988, Reinterpretation of the relationships of the western extension of the Palisades sill to the lava flows at Ladentown, New York, based on new core data, *in* Froelich, A.J., and Robinson, G.R., eds., Studies of the early Mesozoic basins of the eastern United States: U.S. Geological Survey Bulletin 1776, p. 113–135.

Raup, D.M., and Sepkoski, J.J., Jr., 1984, Periodicity of extinctions in the geologic past: Proceedings of the National Academy of Sciences of the United States of America, v. 81, p. 801–805.

Renne, P.R., Swisher, C.C., Deino, A.L., Karner, D.B., Owens, T.L., and DePaolo, D.J., 1998, Intercalibration of standards, absolute ages and uncertainties in $^{40}Ar/^{39}Ar$ dating: Chemical Geology, v. 145, p. 117–152.

Sepkoski, J.J., Jr., 1996, Patterns of Phanerozoic extinction: A perspective from global data bases, *in* Walliser, O.H., ed., Global events and event stratigraphy in the Phanerozoic: Berlin, Springer-Verlag, p. 35–51.

Signor, P.W., and Lipps, J.H., 1982, Sampling bias, gradual extinction patterns and catastrophes in the fossil record, *in* Silver, L.T., and Schultz, P.H., eds., Geological implications of impacts of large asteroids and comets on the Earth: Geological Society of America Special Paper 190, p. 291–296.

Silvestri, S.M., and Szajna, M.J., 1993, Biostratigraphy of vertebrate footprints in the Late Triassic section of the Newark basin, Pennsylvania: Reassessment of stratigraphic ranges, *in* Lucas, S.G., and Morales, M., eds., The nonmarine Triassic: New Mexico Museum of Natural History and Science Bulletin 3, p. 439–445.

Smith, P.L., Tipper, H.W., Taylor, D.G., and Guex, J., 1988, An ammonite zonation for the Lower Jurassic of Canada and the United States: The Pliensbachian: Canadian Journal of Earth Sciences, v. 25, p. 1503–1523.

Smith, P.L., Beyers, J.M., Carter, E.S., Jakobs, G.K., Pálfy, J., Pessagno, E., and Tipper, H.W., 1994, North America, Lower Jurassic, *in* Westermann, G.E.G., and Riccardi, A.C., eds., Jurassic taxa ranges and correlation charts for the Circum Pacific: Newsletters on Stratigraphy, v. 31, p. 33–70.

Taylor, A.S., and Lasaga, A.C., 1999, The role of basalt weathering in the Sr isotope budget of the oceans: Chemical Geology, v. 161, p. 199–214.

Taylor, D.G., Boelling, K., Holser, W.T., Magaritz, M., and Guex, J., 1992, Ammonite biostratigraphy and geochemistry of latest Triassic and earliest Jurassic strata from the Gabbs and Sunrise Formations, Nevada: Geological Society of America Abstracts with Programs, v. 24, p. 85.

Veizer, J., Ala, D., Azmy, K., Bruckschen, P., Buhl, D., Bruhn, F., Carden, G.A.F., Diener, A., Ebneth, S., Godderis, Y., Jasper, T., Korte, C., Pawellek, F., Podlaha, O.G., and Strauss, H., 1999, $^{87}Sr/^{86}Sr$, $\delta^{13}C$ and $\delta^{18}O$ evolution of Phanerozoic seawater: Chemical Geology, v. 161, p. 59–88.

Vörö, A., 1993, Jurassic brachiopods from the Bakony Mts. (Hungary): Global and local effects on changing diversity, *in* Pálfy, J., and Vörös, A., eds., Mesozoic brachiopods of Alpine Europe: Budapest, Hungarian Geological Society, p. 179–187.

Ward, P.D., Haggart, J.W., Carter, E.S., Wilbur, D., Tipper, H.W., and Evans, T., 2001, Sudden productivity collapse associated with the Triassic-Jurassic boundary mass extinction: Science, v. 292, p. 1148–1151.

Zachos, J.C., Arthur, M.A., and Dean, W.E., 1989, Geochemical evidence for suppression of pelagic marine productivity at the Cretaceous Tertiary boundary: Nature, v. 337, p. 61–64.

MANUSCRIPT ACCEPTED BY THE SOCIETY MARCH 22, 2001

Printed in the U.S.A.